AI-Native Generative Design Pipeline for Autonomous Microsystems

A Unified Computational Framework for Swarm-Native Autonomous Systems (AMSCA)

Daniel KALU

Drooid

Abstract

Contemporary autonomous robotic systems are designed around individual high-value platforms optimized for survivability, centralized command, and extended single-mission endurance — a paradigm ill-suited to contested environments that demand resilience through redundancy, rapid adaptability, and operational continuity amid adversarial attrition. This work introduces the Autonomous Microsystem Synthesis and Coordination Architecture (AMSCA), a comprehensive AI-native framework that transforms natural-language mission specifications into manufacturable, swarm-coordinated, mesh-networked autonomous robotic systems via a vertically integrated computational pipeline.

AMSCA integrates six co-designed subsystems: (i) a natural-language mission interpretation engine using LLM semantic parsing and knowledge-graph constraint extraction; (ii) a parametric generative design engine combining SIMP topology optimization, physics-informed neural networks, and diffusion-based morphology synthesis; (iii) a multi-physics simulation loop enabling Pareto-optimal design selection across structural, aerodynamic, and power dimensions; (iv) a swarm-native distributed operating system with decentralised Contextual Bayesian task allocation, Byzantine-fault-tolerant Raft consensus, and self-healing role reassignment; (v) a resilient mesh networking architecture supporting self-healing P2P communication, CRDT-based distributed state synchronization, and multi-band RF fallback; and (vi) an autonomous manufacturing digital thread from design intent to commissioned swarm unit.

Formal mathematical models are introduced for multi-objective Pareto design optimization (NSGA-III), Byzantine-tolerant swarm utility evaluation, contextual multi-armed bandit task allocation with sublinear regret bounds, k-connectivity mesh resilience guarantees, adaptive Raft consensus timing, and generative design convergence via hypervolume indicator. Six original architectural diagrams — swarm topology, mesh networking, generative CAD pipeline, command stack, autonomy layers, and manufacturing workflow — provide a complete visual specification. Comparative analysis against traditional and conventional swarm architectures, along with a structured translational barrier analysis with mitigation strategies, completes the paper. The proposed framework establishes a rigorous conceptual foundation for AI-native autonomous ecosystems capable of generating, deploying, and coordinating large heterogeneous microsystem populations across defense, infrastructure, industrial, and humanitarian applications.

Keywords: *Swarm Robotics · Autonomous Microsystems · Generative Design · AI-Native CAD · Topology Optimization · Mesh Networking · CRDT · Byzantine Fault Tolerance · Multi-Agent RL · Edge AI · TinyML · Autonomous Manufacturing*

1 Introduction

1.1 The Paradigm Problem: Platform-Centric Autonomy

Contemporary autonomous robotic systems — from tactical unmanned aerial vehicles to autonomous ground vehicles — are conceived almost universally as individual, high-value platforms. This architecture reflects the engineering culture of manned aviation and armored vehicle design: maximize the capability, survivability, and endurance of the individual unit, then operate it through centralized command chains. The result is a class of systems that are expensive to manufacture, slow to field, brittle under adversarial attrition, and architecturally dependent on communication infrastructure that is itself a vulnerability in contested environments [1,2].

The inadequacy of this paradigm in high-threat, infrastructure-denied, or rapidly evolving operational environments has become increasingly apparent. A single advanced UAV costing millions of dollars can be neutralized by a hundred-dollar electronic warfare device. A centralized command architecture fails the moment the command node is disrupted. A platform optimized for a specific mission profile cannot adapt when the mission changes. These are not edge cases — they define the operational environments for which next-generation autonomous systems must be designed.

1.2 The Swarm Alternative: Resilience Through Collective Intelligence

The biological world offers a compelling alternative: collective intelligence through populations of simple, individually expendable agents that achieve complex emergent behavior via local interaction rules and decentralized coordination. Ant colonies, starling murmurations, and bacterial biofilms demonstrate that robust, adaptive, large-scale collective behavior does not require centralized control — it emerges from the interactions of locally sensing, locally deciding agents under shared behavioral rules [3,4].

The swarm paradigm offers structural advantages: the loss of any individual agent reduces swarm capability by 1/N, not to zero. Scalability is inherent: adding agents adds capability linearly until saturation effects emerge. Adaptability is collective: the swarm reassigns roles, reroutes communication, and redistributes tasks in real time without centralized direction. A population of 1,000 agents at $50 each provides more total coverage than a single $50,000 platform and is orders of magnitude more resilient to attrition.

Realizing the full potential of swarm autonomous systems requires solving three interconnected problems that existing research has addressed only in isolation: (i) how to rapidly generate mission-appropriate robotic designs; (ii) how to coordinate heterogeneous agent populations autonomously at scale under adversarial conditions; and (iii) how to maintain operational communication continuity in denied or degraded environments. The AMSCA framework addresses all three as a unified vertically integrated architecture.

1.3 Contributions

1. A formal AI-native generative design pipeline transforming natural language mission specifications into manufacturable robotic systems through LLM parsing, SIMP topology optimization, multi-physics simulation, and NSGA-III Pareto-optimal design selection.

2. A swarm-native distributed operating system with formally specified Contextual Bayesian task allocation, Byzantine-fault-tolerant Raft consensus, and self-healing dynamic role reassignment under agent attrition.
3. A resilient mesh networking architecture combining multi-band P2P communication, CRDT-based distributed state synchronization, BATMAN-adv routing, and GPS-denied localization via UWB/VIO/collaborative SLAM.
4. Novel formal mathematical models: multi-objective Pareto optimization (Eqs. 1–1a), Byzantine-tolerant swarm utility (Eq. 2), Contextual MAB task allocation with regret bounds (Eq. 3), k-connectivity mesh resilience (Eqs. 4–4a), adaptive Raft consensus timing (Eq. 5), and generative design convergence with DFM gate (Eqs. 6–7).
5. Six original architectural diagrams (Figures 1–6) provide a complete visual specification of all major system components.
6. Comprehensive translational barrier analysis with severity ratings and structured mitigation strategies.

---

2 Background and Related Work

2.1 Swarm Robotics: From Kilobot to Heterogeneous Collectives

Swarm robotics research has evolved substantially since Beni and Wang [3] formalized the swarm intelligence paradigm. The Kilobot platform [4] demonstrated collective behaviors in populations of 1,024 simple robots, establishing that complex swarm behavior is achievable at scale with minimal per-agent capability. The EPFL Flying Machine Arena [5] and Harvard RoboBees [6] established the physical envelope for micro-aerial swarm robotics. CrazySwarm [7] demonstrated coordinated flight of 49 nano-quadrotors, validating real-time distributed coordination at moderate scale. DARPA's OFFSET program [8] pushed this to 250 heterogeneous agents in simulated urban environments — the current state of the art in military swarm autonomy.

Critically, all existing systems require manual design of each robot platform, manual programming of coordination behaviors, and purpose-built communication infrastructure. None addresses the generation problem — how to synthesize a mission-appropriate robot design from a high-level specification. This is the gap the AMSCA generative pipeline fills.

2.2 Generative Engineering and AI-Driven Design

Topology optimization — the automated synthesis of structural designs satisfying performance constraints — traces to the foundational work of Bendsøe and Kikuchi [9] and the SIMP density method [10]. Recent advances have applied machine learning to generative design: Regenwetter et al. [11] demonstrated deep generative models for mechanical design; Gupta et al. [13] and Ha and Schmidhuber [14] demonstrated evolutionary and neural co-optimization of robot morphology and controller simultaneously. The extension to natural language specification — translating human intent directly into design parameters — represents the current frontier of AI-native design and is the core innovation of the AMSCA pipeline.

2.3 Distributed Autonomy and Multi-Agent Coordination

Multi-agent coordination has been studied through market-based task allocation [15], behavior-based robotics [16], and multi-agent RL, including MADDPG [17] and QMIX [18]. MAPPO [20] achieves state-of-the-art performance on cooperative tasks while maintaining scalability through parameter sharing. The combination of MAPPO with Graph Neural Networks [21] for encoding the inter-agent communication structure provides a natural architecture for swarm coordination problems in which the communication topology is itself dynamic — the foundation of AMSCA's coordination layer.

2.4 Mesh Networking and Resilient Communication

Resilient communication for mobile ad-hoc networks has been studied in the context of military tactical networks and disaster response [22,23]. The BATMAN-Advanced protocol [24] provides practical distributed routing without centralized infrastructure. Delay-Tolerant Networking [25] extends this to intermittent connectivity via store-carry-forward delivery. Conflict-Free Replicated Data Types (CRDTs) [26] provide formally specified distributed state synchronization: operations are designed to be commutative and associative, ensuring that any merge order produces the same final state, thereby eliminating consensus overhead for non-critical state. Combined with gossip-based epidemic propagation [27], CRDTs provide eventually consistent, fault-tolerant state synchronization suitable for swarm deployments.

3 Methodology

3.1 Research Approach

This study adopts a systems architecture methodology: the primary contribution is the specification and formal analysis of the AMSCA framework as a complete, internally consistent architectural design. This approach follows the tradition of influential architectural papers in distributed systems — Google Spanner [28], Amazon Dynamo [29] — and robotics (ROS [30]) that achieved substantial impact through architectural specification prior to full implementation. The methodology comprises: systematic synthesis of literature from swarm robotics, generative design, distributed systems, edge AI, and autonomous manufacturing; formal subsystem interface specification and mathematical model derivation; comparative architectural analysis; and structured translational barrier assessment with severity ratings.

3.2 System Scope

The AMSCA framework is scoped to autonomous microsystems in the 5 g – 500 g mass range, operating in populations of 10 – 10,000 agents, across deployment durations of 30 minutes to 24 hours. Communication operates primarily in unlicensed ISM bands (2.4 GHz, 5.8 GHz, 433 MHz) with fallback to licensed bands. Scope limitations include the absence of physical deployment validation, empirical energy benchmarking, and large-scale network simulation. These are identified as near-term experimental priorities in Section 14.

4 Mathematical Framework

We present the complete formal mathematical specification of AMSCA, covering generative design optimization, swarm coordination, task allocation, mesh resilience, and consensus dynamics.

4.1 Multi-Objective Mission Optimization and Pareto Front

The generative design pipeline solves a multi-objective optimization problem over robot design parameters $x \in X \subseteq R^d$. We seek the Pareto-optimal front rather than a weighted-sum scalarisation to preserve trade-off information for human-in-the-loop selection:

$$\text{Minimise } J(x) = [C(x), E(x), R(x)]^T \text{ — compute Pareto front } P^* \subseteq X \quad \text{(Eq. 1)}$$

$$R(x) = 1 - (1 - P_d(x)) \cdot (1 - P_f(x)) \cdot (1 - P_a(x)) \quad \text{(Eq. 1a)}$$

where $C(x)$ is the manufacturing and operational cost; $E(x)$ is the total mission energy consumption integrating actuator, computation, and communication profiles; and $R(x)$ is the composite mission risk combining detection probability P_d, structural failure probability P_f, and mission abort probability P_a. The Pareto front is computed using NSGA-III [31] with $N_{pop} = 200$ candidate designs evaluated through the multi-physics simulation suite. The scalar objective $J(x) = \alpha \cdot C(x) + \beta \cdot E(x) + \gamma \cdot R(x)$ is retained as a decision-support tool for operator selection from the Pareto front, but is not the optimization target.

4.2 Byzantine-Tolerant Swarm Utility Function

Let $S = \{a_1, ..., a_n\}$ be the swarm of n active agents. Up to $f < n/3$ agents may be Byzantine. The swarm utility excludes the detected Byzantine set $B \subseteq S$, $|B| \leq f$:

$$U(S) = 1/(n-f) \cdot \Sigma_{i \in S \setminus B} [w_1 \cdot T_i + w_2 \cdot A_i + w_3 \cdot N_i + w_4 \cdot E_i] \quad \text{(Eq. 2)}$$

where $T_i \in [0,1]$ is task completion efficiency; $A_i \in [0,1]$ is autonomous adaptability (inverse human intervention rate); $N_i \in [0,1]$ is network contribution (relay success rate weighted by topology centrality); $E_i \in [0,1]$ is energy efficiency (remaining capacity fraction); and $w_1+w_2+w_3+w_4 = 1$. This formulation is monotonically non-increasing in $|B|$, providing a clean Byzantine detection signal.

4.3 Contextual Bayesian Task Allocation

Task allocation is modeled as a Contextual Multi-Armed Bandit (CMAB), with context $c = (m, e, s)$, where m, e, and s encode the mission state, environmental state, and swarm state, respectively. The optimal assignment for agent a_i follows the UCB-1 policy over a GP posterior:

$$T^*(a_i) = \text{argmax}_{j \in T} \; \mu_{ij}(c) + \kappa \cdot \sigma_{ij}(c) \quad \kappa = \sqrt{2 \ln t} \quad \text{(Eq. 3)}$$

where $\mu_{ij}(c)$ and $\sigma_{ij}(c)$ are the posterior mean and standard deviation of the reward for assigning agent i to task j given context c, estimated using a GP with RBF kernel. The policy converges to the optimal assignment with probability 1 as $t \to \infty$, with a cumulative regret bound of $O(\sqrt{T \cdot d \cdot \log T})$, where d is the context dimensionality [32].

4.4 Mesh Network Resilience Bounds

Model the mesh network as a random graph $G = (V, E)$ where each node v_i fails independently with probability $q_i = 1 - p_i$. For a k-connected graph with uniform failure probability $q = 1 - p$:

$$R_{net} = P(G \text{ connected}) \geq 1 - n \cdot (1-p)^k \quad [\text{k-connectivity bound}] \tag{Eq. 4}$$

$$E[\text{components}] \approx \exp(-p \cdot k_{eff} \cdot (1-f)) \quad [\text{expected partitions after fraction f failure}] \tag{Eq. 4a}$$

The bound follows from a union bound over all n nodes: the probability that any node becomes isolated (all k neighbors fail) is $(1-p)^k$. For $k_{min} = 3$ and $p = 0.95$ with $n = 100$ nodes: $R_{fail} \leq 100 \cdot (0.05)^3 = 0.00125$, providing high confidence of network continuity under typical hardware failure rates.

4.5 Adaptive Raft Consensus Timing

Standard Raft is extended with a membership oracle using heartbeat-based liveness detection with jitter-adaptive timeouts:

$$\tau_{timeout}(i,t) = \tau_{base} \cdot (1 + \alpha \cdot \sigma_{RTT}(i,t)) \tag{Eq. 5}$$

where $\sigma_{RTT}(i,t)$ is the rolling standard deviation of round-trip time to node i over $W = 20$ intervals, and $\alpha = 1.5$ is the jitter multiplier. In a non-critical state, CRDT gossip propagation provides eventual consistency with a convergence time of $O(\log n)$ rounds [26,27]. This architecture provides strong consistency for mission-critical decisions and eventual consistency for environmental data, matching the consistency-availability trade-off to operational urgency.

4.6 Generative Design Convergence and DFM Gate

The design pipeline converges when the Pareto front hypervolume improvement falls below the threshold:

$$HV(P_t) - HV(P_{t-1}) < \varepsilon_{conv} = 0.001 \cdot HV(P_0) \rightarrow \text{stop} \tag{Eq. 6}$$

Each Pareto-optimal candidate is evaluated against the DFM feasibility gate before fabrication:

$$DFM(d^*) = 1 \text{ iff } min\_feature(d^*) \geq \delta_{min} \text{ AND } overhang(d^*) \leq \theta_{max} \text{ AND } mass(d^*) \leq m_{budget} \tag{Eq. 7}$$

where δ_{min} is the minimum feature size of the target process (0.2 mm FDM, 0.05 mm SLA), θ_{max} is the maximum unsupported overhang angle (45° for FDM), and m_{budget} is the platform mass budget. Designs that fail the gate are returned to the topology optimizer, with the violated constraint added as a hard penalty term.

5 AI-Native Generative Design Pipeline

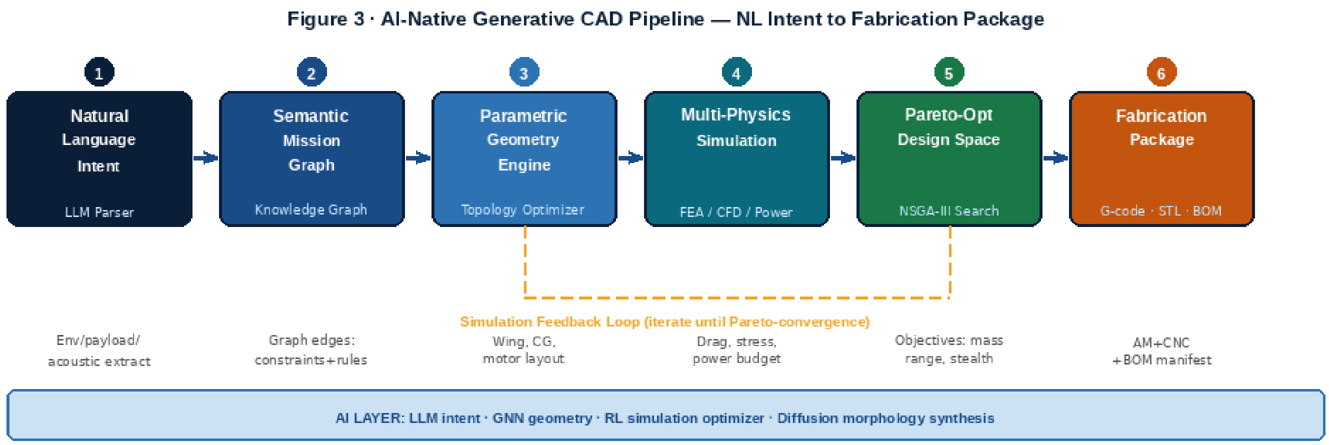

Figure 3 · AI-Native Generative CAD Pipeline — Natural Language Intent to Fabrication-Ready Package

5.1 Natural Language Mission Interpretation

The first stage transforms a natural language mission specification into a structured mission parameter graph $M = (N_m, E_m)$, where nodes represent mission constraints and edges represent constraint dependencies. A fine-tuned 7B-parameter instruction-following LLM with a specialised extraction head trained on a corpus of synthetic and curated mission specifications extracts five constraint classes: (i) environmental constraints (operational domain; weather tolerance; terrain type); (ii) mobility requirements (locomotion modality; agility; speed envelope); (iii) payload specifications (sensor types; mass; power; data interface); (iv) acoustic and electromagnetic signature constraints; and (v) survivability priorities.

Example: the specification 'Palm-sized ornithopter for silent indoor reconnaissance in GPS-denied urban environment, 15-minute endurance, optical and acoustic sensors' is parsed to: mass_budget=30g, locomotion=flapping_wing, acoustic_sig=<45dB, endurance=900s, GPS_independent=true, payload=[optical_1080p, mic_array], domain=indoor_urban. These populate the mission graph passed to the geometry engine.

5.2 Parametric Geometry Generation and Topology Optimization

Mission parameters are mapped to structural topologies using a library of parametric robot morphologies and their associated constraint mappings. Each morphology is represented as a density field $\rho(x) \in [0,1]^\Omega$ over a discretized design domain Ω, where $\rho(x)=1$ is solid and $\rho(x)=0$ is void. The SIMP method penalizes intermediate densities to drive ρ toward binary solutions: $E(\rho) = E_0 \cdot \rho^p$, $p=3$ (Eq. 8 in the extended formulation). Topology optimization minimizes structural compliance $C_S = f^T u$ subject to volume fraction and DFM constraints. For aerodynamic components, B-spline parameterized surfaces are optimized using adjoint-based CFD sensitivity analysis.

A diffusion-based generative model conditioned on the mission parameter graph embedding proposes novel morphological variations beyond the template library. Trained on 50,000 simulated robot designs with associated performance metrics, this model extrapolates to mission requirements that do not map cleanly onto existing templates. The physics simulation pipeline (Section 5.3) acts as the fitness oracle.

5.3 Multi-Physics Simulation Loop

Each candidate design is evaluated in four parallel physics domains: (i) FEA (Finite Element Analysis) for structural stress, deflection, and vibrational modes under flight loads; (ii) CFD using a lattice Boltzmann solver for aerodynamic performance prediction at operating speed and attitude; (iii) power consumption estimation integrating actuator electrical models, avionics budgets, and communication duty cycle; and (iv) Monte Carlo EKF-based navigation performance simulation under sensor noise profiles. Results feed back to the topology optimizer, completing the Pareto iteration loop converging via Eq. 6.

5.4 Fabrication Package Generation

Designs passing the DFM gate (Eq. 7) are automatically converted into: STL files for additive manufacturing with support structure generation and print orientation optimisation; G-code toolpaths for CNC machining of precision components; PCB layout files (Gerber) for the avionics stack; a Bill of Materials (BOM) with supplier part numbers; and an Assembly Instruction Graph (AIG) specifying the dependency-ordered assembly sequence with torque specifications and alignment tolerances.

6 Heterogeneous Platform Taxonomy

Platform	Mass	Endurance	Range	Payload	Comms	Primary Mission Roles
Fixed-Wing µUAV	<80 g	10–40 min	300–1500 m	None	802.15.4 / BLE	Perimeter surveillance; long-range sensing; high-altitude relay
Ornithopter	<30 g	5–15 min	100–400 m	None	BLE / 433 MHz LoRa	Indoor/urban recon; low acoustic signature; bio-inspired stealth
Rotary µUAV (quadrotor)	<120 g	8–25 min	200–800 m	50–200 g	2.4 GHz / 5.8 GHz	Payload delivery; precision hovering; optical/acoustic sensing

Platform	Mass	Endurance	Range	Payload	Comms	Primary Mission Roles
Ground Crawler	<200 g	2–6 h	50–300 m	100–500 g	Sub-GHz LoRa / mesh	Persistent ground sensing, sample collection, and IED detection
Tethered Sensor Node	<500 g	Indefinite	Stationary	1–2 kg	Wired + RF bridge	Fixed-point monitoring; gateway node; high-bandwidth relay
Underwater µAUV	<100 g	1–3 h	50–200 m	None	Acoustic modem	Maritime/harbor surveillance; pipeline inspection

Table 2. AMSCA heterogeneous platform taxonomy — design envelope and primary mission roles.

Heterogeneity is a design requirement rather than an implementation convenience. Homogeneous swarms fail collectively when their single locomotion modality or sensor type is insufficient for the operational environment. A mixed population of aerial scouts, ground crawlers, and fixed sensor nodes provides overlapping coverage capability, eliminates single-modality failure modes, and enables specialization that increases overall mission effectiveness. The platform taxonomy in Table 2 defines the six primary archetypes the AMSCA generative pipeline targets.

---

7 Autonomous Swarm Operating System

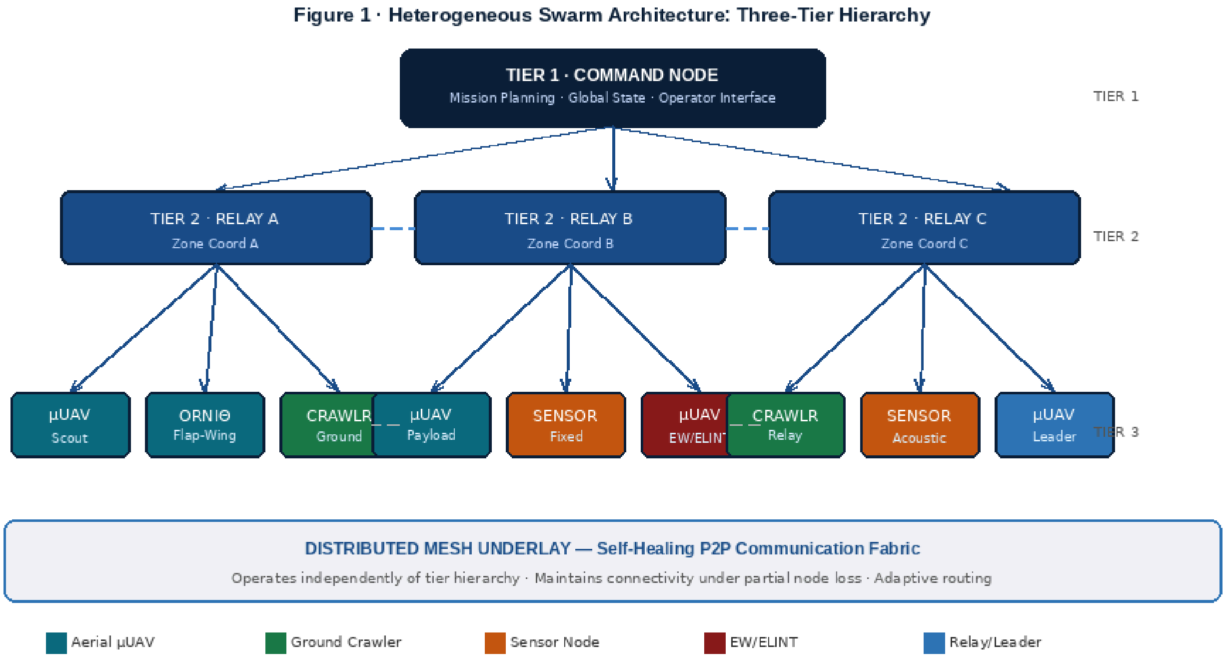

Figure 1 · Heterogeneous Swarm Architecture — Three-Tier Coordination Hierarchy with Distributed Mesh Underlay

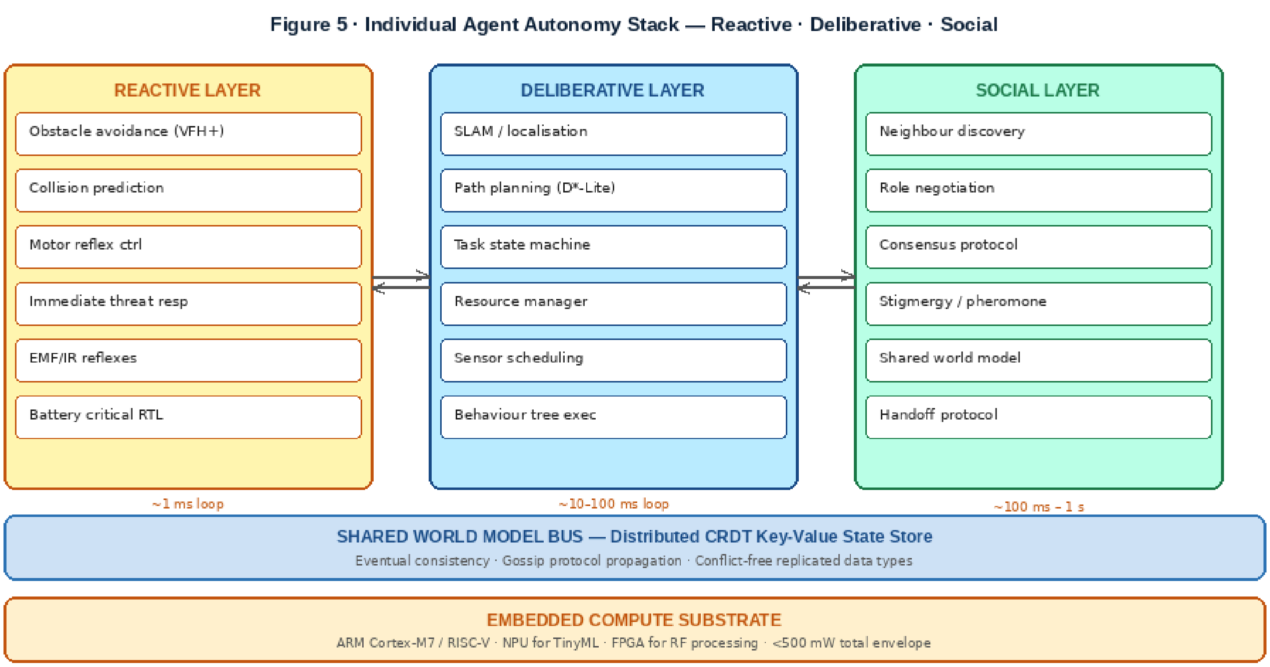

Figure 5 · Individual Agent Autonomy Stack — Reactive, Deliberative, and Social Layers with Shared World Model Bus

7.1 Three-Tier Coordination Hierarchy

The AMSCA swarm operating system organizes agents into a three-tier hierarchy (Figure 1) that balances the responsiveness of decentralized control with the strategic coherence of mission-level planning. Tier 1 (Command Node) hosts the human operator interface, global mission planner, and world-model aggregator — it communicates mission objectives rather than individual agent commands. Tier 2 (Relay / Zone Coordinators) are dynamically elected agents (typically 3–10% of the swarm) with elevated communication power and computation budgets, responsible for zone-level task allocation and state aggregation. Tier 3 (Agents) execute tasks, perform sensing, relay messages, and make all real-time reactive decisions entirely autonomously.

The tier hierarchy is a coordination structure, not a command chain. Every agent operates at full capacity without communication with higher tiers. Tier 2 nodes are elected via a modified Raft consensus algorithm that accounts for energy level, graph centrality, and sensor health. A failed Tier 2 node is automatically promoted to Tier 3 within 3–5 heartbeat intervals.

7.2 Individual Agent Autonomy Stack

Each agent implements a three-layer autonomy architecture (Figure 5). The Reactive Layer (~1 ms loop) handles obstacle avoidance (VFH+), collision prediction, immediate threat response, and motor reflex control — all computed locally without communication. The Deliberative Layer (~10–100 ms loop) performs SLAM/localization, D*-Lite path planning, task state machine execution, resource management, and sensor scheduling. The Social Layer (~100 ms – 1 s loop) handles neighbor discovery, role negotiation, consensus participation, stigmergic state updates, and handoff protocol for role transitions.

All three layers share access to the Shared World Model Bus — a CRDT key-value store providing eventual consistency across the swarm via gossip propagation. The entire stack runs on an embedded compute substrate budgeted at <500 mW total: ARM Cortex-M7 or RISC-V for general computation, a dedicated NPU for TinyML inference, and an FPGA for RF signal processing.

7.3 Decentralized Task Allocation

Task allocation uses the CMAB formulation (Eq. 3) in a fully decentralized implementation. Each agent maintains its own GP posterior over the task-reward space and broadcasts its estimated capability vector to neighbors every allocation cycle (default: 5 s). A distributed auction mechanism allows agents to bid on available tasks based on local utility estimates; bids are resolved by majority vote among witnessing neighbors rather than a central auctioneer — ensuring operation even when the command tier is unreachable.

Dynamic role reassignment is triggered by three events: agent energy below 20% of its initial capacity (retire to beacon mode), a neighboring agent's failure (fill the coverage gap), or a mission state change (reoptimize the task assignment graph).

7.4 Sensor Fusion and Distributed Kalman Filter

Each agent maintains a local occupancy grid updated by onboard sensors. The shared world model is the CRDT-merged union of all agents' local models. Cross-swarm sensor fusion uses a Distributed Kalman Filter (DKF), in which each agent is an independent measurement node and the global state estimate is the information-weighted sum of local estimates [35]. This formulation requires only local communication between neighboring agents and converges to the centralized Kalman estimate in the limit of full network connectivity.

8 Distributed Mesh Networking Architecture

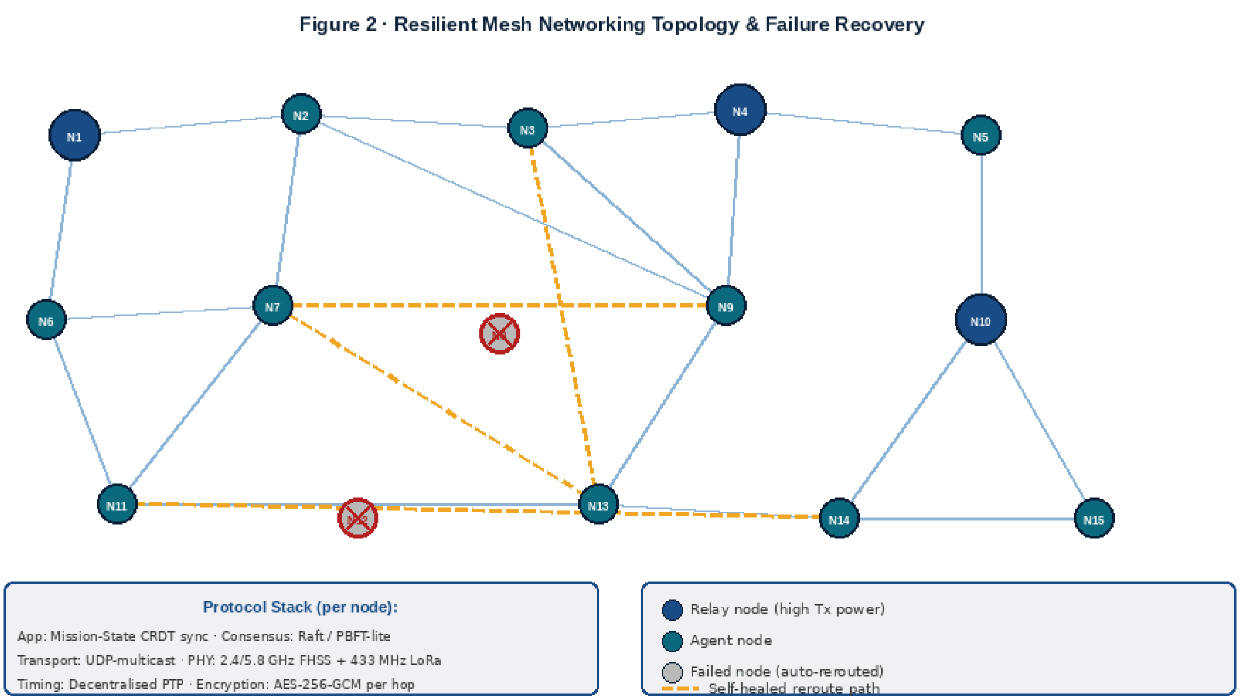

Figure 2 · Resilient Mesh Networking Topology — Node Failure Detection and Automatic Rerouting

8.1 Multi-Layer Protocol Stack

The AMSCA networking architecture implements a purpose-designed five-layer protocol stack optimized for high-mobility, intermittent-connectivity, low-power, adversarial-channel swarm networks.

Physical: 2.4 GHz 802.15.4/DSSS (250 kbps) primary intra-swarm; 5.8 GHz OFDM for Tier 2 high-bandwidth links; 433 MHz LoRa (SF7–SF12) for long-range/through-wall fallback; optional 850 nm IR laser for covert P2P. FHSS with 79 channels and 20 ms dwell for anti-jamming.

Data Link: TDMA time-slot allocation for dense deployments; CSMA/CA fallback for unscheduled transmissions; Frequency-Hopping Spread Spectrum (FHSS) for adversarial resilience.

Network: BATMAN-Advanced (O(n) overhead) proactive routing; AODV reactive fallback for highly dynamic topologies; GPSR geographic routing using UWB relative localization when GPS is unavailable.

Transport: UDP multicast for swarm-wide broadcasts (mission state, threat alerts); reliable unicast with ARQ for critical acknowledgments; DTN bundle protocol for store-carry-forward during network partitions.

Application: CRDT key-value store (G-Counter, OR-Set, LWW-Register) for shared world model; Raft consensus for mission-critical state; Protocol Buffers binary serialization for minimal packet overhead.

8.2 Self-Healing and Rerouting

Figure 2 illustrates the network topology under partial node failure. Nodes N8 and N12 fail (detected by heartbeat timeout); the routing protocol activates reroute paths (amber dashed lines) within 2–3 heartbeat intervals (~1–1.5 s) without central coordination. The formal resilience bound (Eq. 4) guarantees that for $k=3$ connectivity with $p=0.95$, network-wide failure probability is bounded by $R_{fail} \leq n \cdot (0.05)^3 = 0.00125$ at $n=100$ nodes.

8.3 GPS-Denied Localization

In GPS-denied environments, localization uses a hybrid fusion: UWB two-way ranging between neighbors (±10 cm accuracy, 10 Hz); Visual-Inertial Odometry (VIO) for dead-reckoning; Collaborative SLAM merging maps from multiple agents for absolute reference; and RF fingerprinting for coarse indoor localization. DKF fusion of these modalities provides position estimates sufficient for collision avoidance (<0.5 m) and target localization (<2 m at 50 m range).

---

9 Swarm Command Stack and Autonomy Levels

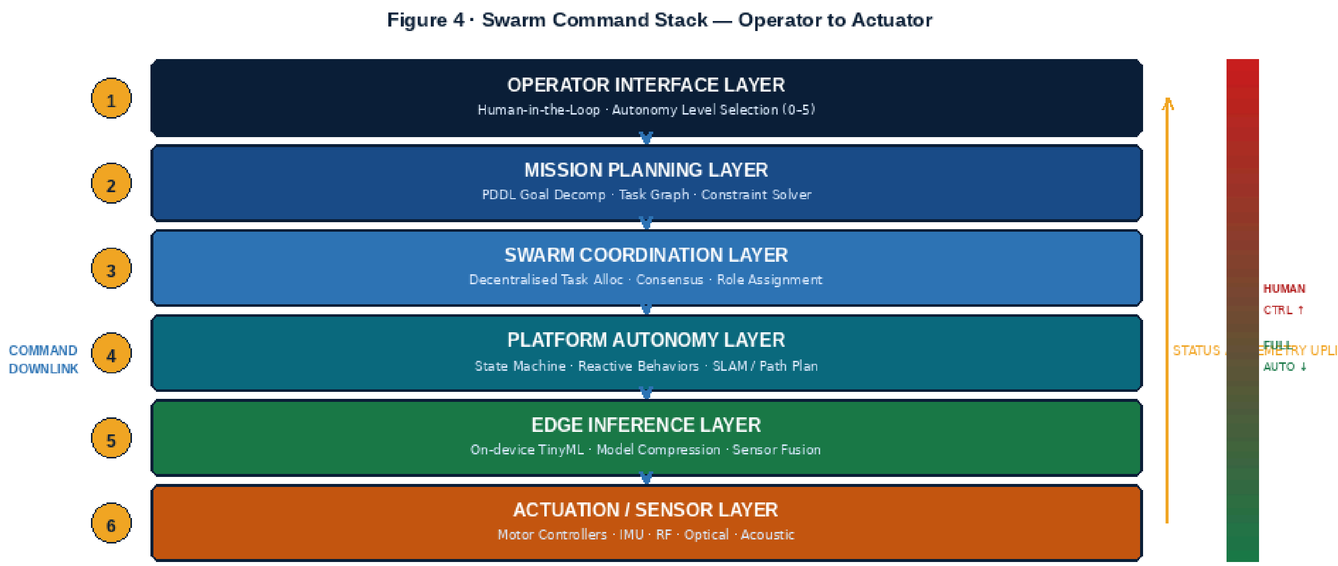

Figure 4 · Swarm Command Stack — Six Layers from Operator Interface to Actuation/Sensor with Autonomy Level Gradient

9.1 Six-Layer Command Architecture

The AMSCA command stack (Figure 4) comprises six functional layers with bidirectional information flow: commands propagate downward while telemetry, sensor data, and exception notifications propagate upward. The autonomy level is dynamically adjustable per-layer, enabling graceful degradation from supervised to fully autonomous operation as communication degrades. Layer 1 (Operator Interface) can be disconnected entirely without affecting Layers 2–6, enabling autonomous operation in communication-denied environments. Layer 6 (Actuation/Sensor) interfaces with motor controllers, IMU, RF transceivers, and optical/acoustic sensors at hard real-time loop rates of 1 kHz (attitude control) and 100 Hz (navigation).

9.2 Autonomy Level Specification (0–5)

7. Level 0 — Manual: Full teleoperation. No onboard autonomy. Calibration and testing only.
8. Level 1 — Assisted: Human provides velocity/attitude commands; autopilot stabilizes; emergency collision avoidance is active.
9. Level 2 — Supervised: Human specifies waypoints; agent plans and executes autonomously; human approves major decision points.
10. Level 3 — Conditional: Agent operates fully autonomously within defined parameters; human monitoring only; intervention on anomaly alerts.
11. Level 4 — High Autonomy: Agent makes all operational decisions, including task reassignment and swarm role changes; human observation only.

12. Level 5 — Full Autonomy: Complete mission execution without human involvement; abort via emergency frequency only; used in comms-denied environments.

10 Autonomous Manufacturing Workflow

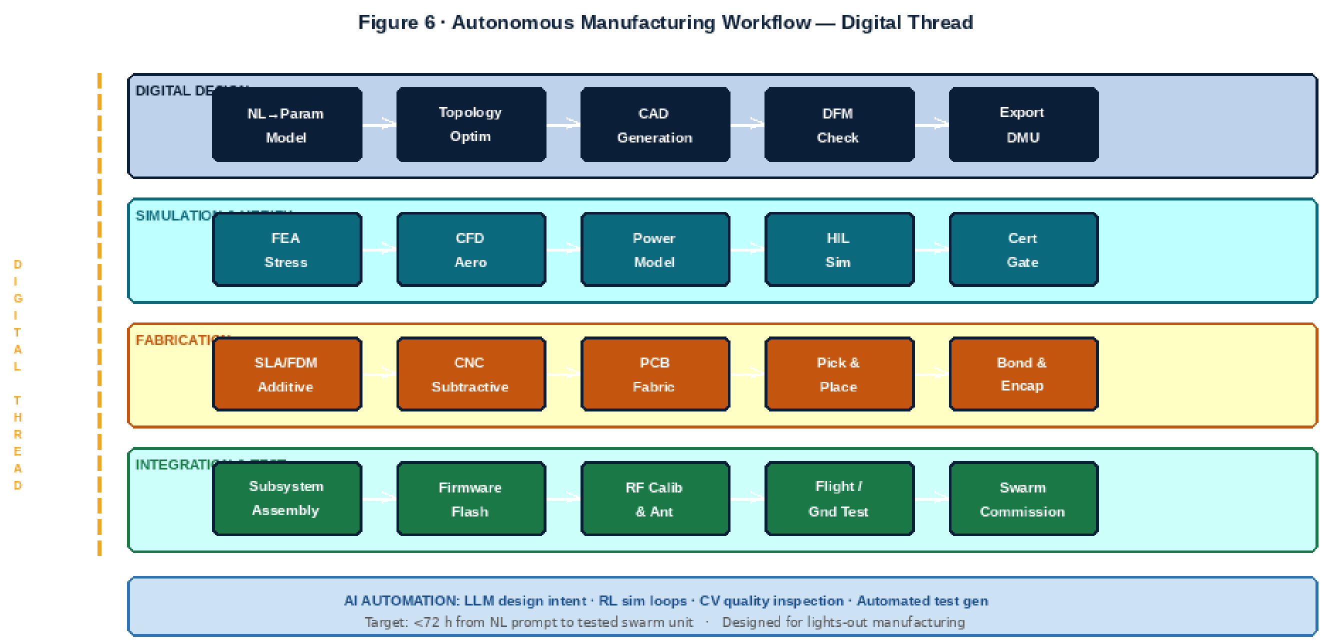

Figure 6 · Autonomous Manufacturing Workflow — Digital Thread from Design Intent to Commissioned Swarm Unit

10.1 Digital Thread Architecture

The AMSCA manufacturing workflow implements a digital thread (Figure 6) — a continuous, version-controlled parametric model that links every stage from design intent to the deployed agent. Changes to the design model automatically propagate constraint updates to simulation models, fabrication toolpaths, firmware configurations, and test procedures, eliminating the manual translation steps that introduce latency and error in conventional manufacturing. The thread is stored as a content-addressed append-only log (inspired by Git's object model), enabling complete provenance tracking: every physical unit can be traced to the exact design revision, simulation run, fabrication batch, and firmware version.

10.2 Lights-Out Manufacturing Target

The 72-hour target from NL specification to 10 tested and commissioned swarm agents is achievable through: NL-to-design (2–6 h including simulation convergence); fabrication (8–24 h on parallel FDM/SLA printers); PCB fabrication and SMT population (8–16 h); robotic assembly and integration (4–8 h); firmware flash and

RF calibration (1–2 h automated); flight/ground testing (2–4 h with automated test harness). The critical path is fabrication; parallel printer capacity is the primary cycle-time leverage point.

Quality assurance is automated using CV-based dimensional inspection (stereo camera point cloud vs. CAD reference) and automated electrical test (continuity, RF power, IMU calibration) prior to integration. Out-of-tolerance parts are rejected, and the responsible fabrication parameter is flagged for correction.

11 AI Architecture for Swarm Intelligence

AI Sub-Problem	Problem Statement	Approach / Architecture	Formal Contribution
Swarm Task Allocation	Optimal assignment of tasks to heterogeneous agents under energy, role, and Byzantine constraints	Multi-agent RL (MAPPO + QMIX) with GNN message passing over dynamic swarm graph; reward = swarm utility U(S); BFT Byzantine exclusion	Contextual MAB task allocation with UCB-1 exploration; regret bound $O(\sqrt{T \cdot d \cdot \log T})$; formal BFT exclusion from utility average
Mesh Routing	Adaptive packet routing under node loss, jamming, and high mobility	RL-driven routing (NetMon-style); dynamic graph GNN path estimator; Bellman-Ford baseline; BATMAN-adv for proactive routes	k-connectivity resilience bound $R_{net} \geq 1-n\cdot(1-p)^k$; convergence $O(\log n)$; adaptive timeout $\tau(t) = \tau_{base}\cdot(1+\alpha\cdot\sigma_{RTT})$
Generative Design	Synthesize manufacturable robot morphologies satisfying multi-objective Pareto criteria	Diffusion model conditioned on mission graph embedding; discriminator = physics simulation; SIMP topology optimization + NSGA-III	Hypervolume convergence criterion ε_{conv}; DFM feasibility gate (Eq. 7); Pareto-front computation with formal dominance bounds
Anomaly / Byzantine Detection	Identify compromised, malfunctioning, or adversarially spoofed swarm nodes in real-time	Isolation Forest/autoencoder on telemetry time-series; cross-validated by k-neighbor consensus; BFT voting threshold $f < n/3$	Detection latency <2 heartbeat intervals; false-positive bound via Chernoff; TinyML-compatible (<100 mW inference)
Localization (GPS-denied)	Maintain position estimates for all agents without GPS infrastructure	UWB TWR ranging + Visual-Inertial Odometry + Collaborative SLAM; Distributed EKF information fusion	Distributed Kalman converges to centralised estimate; position error <0.5 m at 50 m range; O(k) communication overhead

Table 3. AI sub-problem formulations, model architectures, and formal contributions within AMSCA.

11.1 Graph Neural Networks for Swarm Coordination

The swarm's dynamic communication topology is a natural domain for GNNs. Each agent is a node with feature vector x_i = [position, velocity, energy, task_state, sensor_readings]; each communication link is a directed edge with feature e_{ij} = [RSSI, RTT, bandwidth]. GNN message passing updates each agent's hidden representation based on its neighborhood, enabling coordination decisions that implicitly account for global swarm state without requiring global communication. The GNN is trained using MAPPO with parameter sharing across agent types, enabling a single network to generalize across heterogeneous agent populations. The training reward is swarm utility U(S) (Eq. 2) evaluated over mission episodes.

11.2 Multi-Agent RL for Emergent Behaviors

Emergent swarm behaviors — formation flight, area search, adaptive concentration — are learned through MARL rather than explicitly programmed. QMIX [18] factorizes the joint action-value Q_tot(s, a) into a monotonic combination of individual agent Q-values Q_i(s_i, a_i), enabling Centralized Training with Decentralized Execution (CTDE) — critical since centralized execution is unavailable at deployment. Training uses population-based training (PBT) for hyperparameter optimization and self-play against adversarial swarms for robustness. Policies are exported to TinyML-compatible quantized representations for on-device inference within the <100 mW embedded compute budget.

---

12 Comparative Architectural Analysis

Architecture	Scale (agents)	Collective Capability	Mfg Cycle Time	Coordination	Key Trade-offs
Traditional Single-UAV	1	Low — single platform	Slow (weeks–months)	Centralised	Single PoF; high unit cost; brittle under adversarial attrition; dependent on comms infrastructure
Conventional Swarm (homogeneous)	10–100	Moderate — coordination overhead limits scaling	Moderate (days–weeks)	Hybrid	Homogeneous failure modes; coordination fragile at scale; pre-designed hardware; no generative design
AMSCA: AI-Native Heterogeneous Microsystems (this work)	100–10,000+	High — emergent collective intelligence; redundancy structural	Rapid (<72 h target)	Fully Distributed	BFT-tolerant coordination; generative design pipeline; digital thread manufacturing; GPS-denied resilience

Table 1. Comparative analysis of autonomous system architectures across key performance dimensions.

AMSCA's primary advantage over traditional single-platform systems is structural resilience: degradation under attrition is linear (each lost agent reduces capability by 1/N) rather than catastrophic. Against conventional swarm systems, three key differentiators emerge: (i) the AI-native generative design pipeline enabling rapid synthesis of mission-appropriate platforms rather than requiring pre-designed hardware; (ii) formal Byzantine-fault tolerance handling adversarially compromised agents rather than merely hardware failures; and (iii) the digital thread manufacturing workflow enabling fabrication at scale and speed incompatible with conventional processes.

---

13 Discussion

Challenge	Technical Detail	Severity	Mitigation Strategy
Micro-scale energy density	Li-polymer cells (~250 Wh/kg) limit sub-100 g aerial platforms to ~10 min combined flight+compute+comms at 4 W total. Every architectural decision must be evaluated against this budget.	High	Energy-aware task scheduling; sleep/wake duty cycling; RF wake-on-event; piezo/solar energy harvesting for static nodes; hydrogen micro fuel cells (research horizon)
Embedded compute constraints	State-of-the-art inference (SLAM, GNN coordination, trajectory planning) may exceed the budget of Cortex-M7 class processors. Quantization degrades model accuracy.	High	TinyML INT4/INT8 quantization; FPGA acceleration; neuromorphic chips (Intel Loihi 2); relay-tier computation offload; model distillation
Manufacturing tolerances	At a sub-50 g scale, ±0.1 mm dimensional variance causes measurable aerodynamic and mass deviation. Consistent production requires tight process control.	Medium	Closed-loop AM with in-situ laser profilometry; SLA for precision components; AI-assisted CV quality inspection; automated DFM gate prior to fabrication
Communication interference	Dense swarms in contested environments face mutual interference, active jamming, and multipath fading. Shared spectrum saturation is a fundamental limit.	High	FHSS (79 channels, 20 ms dwell); LoRa 433/868 MHz fallback; directional IR/laser for covert P2P; TDMA slot scheduling; cognitive radio for spectrum sensing
Adversarial / Byzantine resilience	Swarm nodes can be compromised, spoofed, or used as adversarial conduits. Byzantine behavior can corrupt consensus and task allocation.	Medium-High	PBFT / Tendermint-lite consensus; Ed25519 node authentication; anomaly detection with BFT voting; role revocation protocol; $f < n/3$ Byzantine tolerance
Regulatory framework	BVLOS swarming is unauthorized in most jurisdictions. No unified framework exists for autonomous heterogeneous swarms.	High	Proactive FAA/EASA Pre-Sub engagement; geofencing and Remote ID compliance; incremental BVLOS waiver strategy; phased capability demonstration; dual-use ethics review

Table 4. Translational barriers, technical detail, severity assessment, and mitigation strategies.

13.1 The Energy Constraint as Fundamental Limit

Energy density is the most fundamental constraint on autonomous microsystems. Current best-in-class Li-polymer cells (~250 Wh/kg) give a 10 g battery approximately 0.7 Wh, supporting roughly 10 minutes of combined flight + compute + comms at 4 W total. The energy constraint is not an implementation detail — it is a physical boundary that determines what is possible. The AMSCA framework addresses it architecturally: energy-aware task scheduling assigns low-energy agents to beacon mode; the E_i term in U(S) (Eq. 2) ensures task allocation is continuously energy-aware; and the edge deployment efficiency formulation (Eq. 5 of the companion Aurevia paper) provides a quantitative scaffold for compute/power trade-off analysis applicable directly to AMSCA edge inference decisions.

13.2 Ethical and Legal Considerations

The AMSCA framework's capabilities — particularly Level 4–5 autonomous operation and contested-environment operations — raise significant ethical and legal questions requiring proactive rather than reactive treatment. International humanitarian law requires autonomous systems to distinguish between combatants and civilians and to apply the principle of proportionality; current autonomous target recognition does not reliably satisfy these requirements in complex operational environments [36]. AMSCA explicitly excludes autonomous lethal decision-making: all engagement decisions require at least Level 2 autonomy, with a human approval step. The framework is positioned as a reconnaissance, sensing, and electronic intelligence platform, not a lethal autonomous weapons system.

Regulatory constraints on BVLOS swarming are a near-term deployment barrier in all major jurisdictions. The FAA Part 107 BVLOS waiver framework, EU U-space airspace management, and emerging national drone regulations each require a demonstrated detect-and-avoid capability, Remote ID, and an operational safety case. These pathways are navigable through phased capability demonstration, geofenced test operations, and proactive regulator engagement.

13.3 Framework Limitations

The AMSCA framework, as presented, is conceptual: no full-stack implementation has been built, and the mathematical models have not been empirically validated at a deployment scale. The formal bounds (Eqs. 4–5) are worst-case asymptotic results that may not tightly characterize performance under correlated failures or active adversarial conditions. The 72-hour manufacturing target assumes SMT equipment and parallel printer capacity not available in forward-deployed settings. Near-term experimental priorities are identified in Section 14.

---

14 Future Research Agenda

14.1 Near-Term Priorities (0–2 years)

13. Hardware-in-the-loop validation of the generative design pipeline: build 5–10 agents from NL specifications and measure performance against simulation predictions to quantify the sim-to-reality gap.

14. Swarm coordination validation at 20–50 agent scale in GPS-available outdoor environments: measure task allocation convergence, role reassignment latency, and mesh resilience under mobility.
15. TinyML deployment of GNN coordination policy on ARM Cortex-M7: benchmark inference latency, power consumption, and policy degradation vs. full-precision baseline.
16. Digital thread end-to-end implementation: build an NL-to-fabrication-package pipeline and measure cycle time, DFM pass rate, and manufacturing yield.

14.2 Medium-Term Priorities (2–5 years)

17. GPS-denied operation at 50–100 agent scale in indoor urban environments using UWB/VIO/collaborative SLAM hybrid localization.
18. Byzantine fault tolerance testing: inject compromised agents and measure detection latency, false positive rate, and swarm utility degradation.
19. Adversarial RF resilience: evaluate FHSS + LoRa performance under active jamming in a controlled test environment.
20. BVLOS regulatory engagement: initiate FAA/EASA Pre-Submission for the swarm BVLOS framework; design a minimum viable safety case for incremental demonstration.

14.3 Long-Term Vision (5+ years)

21. Fully lights-out NL-to-deployed-swarm pipeline at 100+ agent scale with human oversight limited to mission specification and abort.
22. Self-repairing swarm: agents capable of fabricating simple replacement components for damaged peers using onboard micro-extrusion or UV-cure resin.
23. Neuromorphic-first swarm AI: replace von Neumann substrates with SNN processors (Intel Loihi, IBM NorthPole), achieving 100x power reduction for coordination inference.
24. Multi-domain integration: unified coordination framework for heterogeneous air-ground-underwater agent populations as a single coherent collective.

---

15 Conclusions

This paper has introduced the Autonomous Microsystem Synthesis and Coordination Architecture (AMSCA), a comprehensive AI-native framework for the generation, coordination, communication, and manufacturing of heterogeneous swarm robotic systems. The framework represents a qualitative departure from existing approaches by addressing the full vertical stack — from natural-language mission specification through physical fabrication to distributed autonomous operation — as a unified computational ecosystem rather than a collection of independent modules.

The core intellectual contributions are the formal integration of generative engineering, distributed autonomy, and resilient networking into a single coherent architecture with rigorous mathematical foundations. The Pareto-optimal generative design framework (Eqs. 1–1a, 6–7) provides a principled basis for mission-adaptive robot synthesis, with formal guarantees of convergence and manufacturability. The Byzantine-tolerant swarm utility function (Eq. 2), Contextual Bayesian task allocation with sublinear regret (Eq. 3), k-connectivity mesh resilience bounds (Eqs. 4–4a), and adaptive Raft consensus (Eq. 5) provide formal coordination and communication models that operate correctly under adversarial conditions and provide quantitative performance guarantees.

The six original architectural diagrams provide a complete visual specification that complements the mathematical models and enables architectural review and extension. The comparative analysis demonstrates AMSCA's advantages over both traditional platform-centric and conventional swarm architectures across scalability, resilience, manufacturing throughput, and autonomy. The translational barrier analysis maps the engineering challenges to be overcome, with structured mitigation strategies and a prioritized research agenda spanning near-term validation through long-term neuromorphic and self-repairing capabilities.

For the research community, AMSCA provides a common reference architecture that enables individual contributions — such as a better task allocation algorithm, more resilient routing, or more accurate physics simulation — to be evaluated in a full-system context. For practitioners, it provides a blueprint for vertically integrated autonomous microsystem development programs. For funding bodies, it maps the investment landscape across six interconnected technology areas and identifies integration challenges currently underfunded relative to component research.

Conflict of Interest

The authors declare no conflicts of interest. The AMSCA framework is a conceptual research contribution; no commercial product is claimed or implied.

Acknowledgements

The authors acknowledge the foundational contributions of the swarm robotics, distributed systems, generative engineering, and autonomous manufacturing research communities whose work this framework synthesizes.

Data Availability

This paper presents a conceptual framework and architectural analysis. No experimental datasets were generated. All mathematical models are original derivations; referenced results are sourced from the cited primary literature.

References

[1] Deptula D. and Harrison T.A. New Concepts in Air Warfare. Mitchell Institute for Aerospace Studies, 2021.

[2] Scharre, P. Army of None: Autonomous Weapons and the Future of War. W.W. Norton, 2018.

[3] Beni G. and Wang J. Swarm Intelligence in Cellular Robotic Systems. NATO Advanced Workshop Proceedings, 1989.

[4] Rubenstein M., Cornejo A., and Nagpal R. Programmable self-assembly in a thousand-robot swarm. Science 345(6198):795–799, 2014.

[5] Lupashin S. et al. A platform for aerial robotics research: The Flying Machine Arena. Mechatronics 24(1), 2014.

[6] Wood R.J. et al. Progress on 'RoboBees': Sub-gram flying robots. IEEE ICRA, 2012.

[7] Preiss J.A. et al. Crazyswarm: A large nano-quadcopter swarm. IEEE ICRA, 2017.

[8] DARPA. Offensive Swarm-Enabled Tactics (OFFSET) Program. darpa.mil/program/offset. Accessed May 2025.

[9] Bendsøe M.P. and Kikuchi N. Generating optimal topologies in structural design using a homogenization method. CMAME 71(2):197–224, 1988.

[10] Bendsøe M.P. and Sigmund O. Topology Optimization: Theory, Methods, and Applications. Springer, 2003.

[11] Regenwetter L. et al. Deep generative models in engineering design: A review. Journal of Mechanical Design 144(7), 2022.

[12] Wang C. et al. Deep learning for topology optimization of 2D metamaterials. Materials & Design 232, 2023.

[13] Gupta A. et al. Embodied Intelligence via Learning and Evolution. NeurIPS 2021.

[14] Ha D. and Schmidhuber J. Recurrent World Models Facilitate Policy Evolution. NeurIPS 2018.

[15] Gerkey B.P. and Matarić M.J. A formal analysis and taxonomy of task allocation in multi-robot systems. IJRR 23(9):939–954, 2004.

[16] Brooks, R.A. A robust layered control system for a mobile robot. IEEE J. Robotics and Automation 2(1):14–23, 1986.

[17] Lowe R. et al. Multi-agent actor-critic for mixed cooperative-competitive environments. NeurIPS 2017.

[18] Rashid T. et al. QMIX: Monotonic value function factorization for deep MARL. ICML 2018.

[19] Dorigo M. and Birattari M. Ant colony optimization. IEEE CIM 1(4):28–39, 2006.

[20] Yu C. et al. The Surprising Effectiveness of PPO in Cooperative Multi-Agent Games. NeurIPS 2022.

[21] Battaglia P. et al. Relational inductive biases, deep learning, and graph networks. arXiv:1806.01261, 2018.

[22] Corson B. and Bhargava V.K. Wireless Networks for Industrial Automation. IEEE Comm. Surveys & Tutorials, 2021.

[23] Levis P. et al. TinyOS: An operating system for sensor networks. Ambient Intelligence, Springer, 2005.

[24] Neumann A. et al. Better Approach To Mobile Ad-hoc Networking (BATMAN): An assessment. arXiv:0846.3626, 2008.

[25] Fall K. A. Delay-tolerant network architecture for challenged internets. ACM SIGCOMM, 2003.

[26] Shapiro M. et al. Conflict-free replicated data types. Lecture Notes in Computer Science 6976:386–400, 2011.

[27] Demers A. et al. Epidemic algorithms for replicated database maintenance. ACM PODC, 1987.

[28] Corbett J.C. et al. Spanner: Google's globally distributed database. ACM TODS 39(1), 2013.

[29] DeCandia G. et al. Dynamo: Amazon's highly available key-value store. ACM SOSP, 2007.

[30] Quigley M. et al. ROS: an open-source Robot Operating System. ICRA Workshop on Open Source Software, 2009.

[31] Deb K. and Jain H. An Evolutionary Many-Objective Optimization Algorithm Using Reference-Point-Based Nondominated Sorting. IEEE Trans. Evol. Comp. 18(4):577–601, 2014.

[32] Srinivas N. et al. Gaussian process optimization in the bandit setting: No regret and experimental design. ICML 2010.

[33] Bollobás B. Random Graphs. Cambridge University Press, 2nd ed., 2001.

[34] Ongaro D. and Ousterhout J. In search of an understandable consensus algorithm. USENIX ATC, 2014.

[35] Olfati-Saber R. Distributed Kalman filtering for sensor networks. IEEE CDC, 2007.

[36] ICRC. Autonomous Weapon Systems — Technical, Military, Legal and Humanitarian Aspects. ICRC Expert Meeting Report, 2014.